A thermoregulation model based on the physical and physiological characteristics of Chinese elderly

Article

Accepted Version

Zhou, S., Ouyang, L., Li, B., Hodder, S. and Yao, R. ORCID: https://orcid.org/0000-0003-4269-7224 (2024) A thermoregulation model based on the physical and physiological characteristics of Chinese elderly. Computers in Biology and Medicine, 172. 108262. ISSN 1879-0534 doi: 10.1016/j.compbiomed.2024.108262 Available at https://centaur.reading.ac.uk/115752/

To link to this article DOI: http://dx.doi.org/10.1016/j.compbiomed.2024.108262

Publisher: Elsevier

A thermoregulation model based on the physical and physiological characteristics of Chinese elderly

Shan Zhou [a, b], Linyuan Ouyang [a, b], Baizhan Li [a, b], Simon Hodder [c], Runming Yao [a, b, d *]

[a] Joint International Research Laboratory of Green Buildings and Built Environments (Ministry of Education), Chongqing University, Chongqing, 400045, China

[b] National Center for International Research of Low-carbon and Green Buildings (Ministry of Science and Technology), Chongqing University, Chongqing, 400045, China

[c] School of Design & Creative Arts, Loughborough University, Loughborough, LE11 3TU, UK

[d] School of the Built Environment, University of Reading, Reading, RG6 6DB, UK

Corresponding author E-mail addresses: r.yao@cqu.edu.cn (Runming Yao)

Abstract

Given the increasing aging population and rising living standards in China, developing an accurate and straightforward thermoregulation model for the elderly has become increasingly essential. To address this need, an existing one-segment four-node thermoregulation model for the young was selected as the base model. This study developed the base model considering age-related physical and physiological changes to predict mean skin temperatures of the elderly. Measured data for model optimization were collected from 24 representative healthy Chinese elderly individuals (average age: 67 years). The subjects underwent temperature step changes between neutral and warm conditions with a temperature range of 25–34˚C. The model's demographic representation was first validated by comparing the subjects' physical characteristics with Chinese census data. Secondly, sensitivity analysis was performed to investigate the influences of passive system parameters on skin and core temperatures and adjustments were implemented using measurement or literature data specific to the Chinese elderly. Thirdly, the active system was modified by resetting the body temperature set points. The active parameters to control thermoregulation activities were further optimized using the TPE (Tree-structured Parzen Estimator) hyperparameter tuning method. The model's accuracy

was further verified using independent experimental data for a temperature range of 18–34˚C for Chinese elderly. By comprehensively considering age-induced thermal response changes, the proposed model has potential applications in designing and optimizing thermal management systems in buildings, as well as informing energy-efficient strategies tailored to the specific needs of the Chinese elderly population.

Keywords

Thermoregulation model; elderly; skin temperature; transient environments; sensitivity analysis; hyperparameter optimization method

Nomenclature

Abbreviations	
ARMSE	Average root mean squared error
BMI	Body mass index
BSA	Body surface area
PMV-PPD	Predicted mean vote and predicted percentage of dissatisfied
RH	Relative humidity, %
RMSE	Root mean square error
TPE	Tree-structured Parzen Estimator
Symbols	
A	Body surface area of the human body, m^2
BF_{s}	The blood flow rate of the skin layer, L/h
BFB_{s}	Basal blood flow at the neutral thermal condition, L/h
c_{bl}	The specific heat of blood, J/(kg·k)
c_i	The specific heat of the *i*th layer, J/(kg·k)
c_j	The specific heat of the *j*th node, J/(kg·k)
C_{dl}	The vasodilation coefficient for the core layer, L/(h·˚C)
C_{res}	Convective heat dissipation, W/m^2
C_{st}	The vasoconstriction coefficient for the core layer, 1/˚C
C_{sw}	The sweating coefficient for the core layer, $W/{}^{\circ}C \cdot m^2$

E_{res}	Evaporative heat dissipation, W/m^2
Err_{c}	The input signal of the core layer, ˚C
Err_{s}	The input signal of the skin layer, ˚C
F_{c}	The temperature change rate of the core layer, ˚C/s
F_{s}	The temperature change rate of the skin layer, ˚C/s
l_{h}	Height of the model, m
M	Metabolic rate, met, 1 met = 58.15 W/m^2
q_i	Thermal production of metabolism of the *i*th layer, W/m^3
q_j	Thermal production of metabolism of the *j*th node, W/m^3
r	The radius to body center, m
r_i	The radius from the *i*th layer to body center, m
r_j	The distance from the *j*th node to the center of the model, m
$r_{s,i}$	Radius of the outer boundary of the *i*th layer, m
$RMSE_{n,gender}$	RMSE of the *n*th condition of males or females, ˚C^2
S_{dl}	The vasodilation coefficient for the skin layer, L/(h·˚C)
S_{st}	The vasoconstriction coefficient for the skin layer, 1/˚C
S_{sw}	The sweating coefficient for the skin layer, W/˚C·m^2
T_{bl}	The temperature of blood, ˚C
T_c	Core temperature, ˚C
T_i	The temperature of the body tissue at the *i*th layer, ˚C
T_j	The temperature of the body tissue at the *j*th node, ˚C
T_s	Skin temperature, ˚C
$T_{set,\mathrm{c}}$	Set point of the core layer at the neutral state, ˚C
$T_{set,s}$	Set point of the skin layer at the neutral state, ˚C
$T_{sk,k}$	The measured mean skin temperature at the *k*th minute, ˚C
$\hat{T}_{sk,k}$	The model output mean skin temperature at the *k*th minute, ˚C
$T_{\tau,j}$	The temperature of the *j*th node at the time τ, ˚C
V_i	Volume of the *i*th layer, m^3
W	External work, W/m^2
w_{bl}	Blood perfusion rate per cubic meter, m^3/(s·m^3)
λ_i	Thermal conductivity coefficient at the *i*th layer, W/(m·k)
λ_j	Thermal conductivity coefficient at the *j*th node, W/(m·k)

ρ_{bl}	The density of blood, kg/m^3
ρ_i	The density of the *i*th layer, kg/m^3
ρ_j	The density of the *j*th node, kg/m^3
Δt	The time interval, s
Δr	The spatial discrete spacing, m
τ	Time, s
$\tau - 1$	The last time, s
Subscripts	
bl	Blood
c	Core layer
dl	Vasodilation
i	The body tissue at the *i*th layer
j	The body tissue at the *j*th node
j+1	The next/downstream node
j−1	The last/upstream node
res	Respiration
s	Skin layer
st	Vasoconstriction
sw	Sweating

1. Introduction

1.1 Background

The aging population is growing worldwide [1,2]. The United Nations predicted that the percentage of the elderly (over 60 years old) in China will reach 30.4% and 38.9% in 2035 and 2050, respectively [3]. The aging society has become a major challenge for economic growth and social care because of the declining capacity of the elderly to work and sustain themselves [1,4]. It has been reported that the elderly spend the majority of their time indoors [5]. However, given the current situation, existing dwelling stocks are not capable of providing enough protection against heat for the elderly in summer [6]. Low air-conditioner use was found in the elderly's dwellings [5,7,8] and overheating in built environments was a rising problem for elderly people due to the increasing frequency and intensity of warm summers [9–11]. One of the causes of indoor overheating in summer is that elderly people have lower abilities to detect high temperatures so their thermal sensation votes are lower than those of non-elderly adults [5,7,12,13]. Thus, they can accept a wider range of indoor temperatures with higher acceptable upper limits which can be higher than 30˚C [12,14–17], surpassing the upper limit of the minimum mortality temperature which ranges from 18–30˚C [18,19]. Given the current situation of unfavorable thermal conditions, the elderly are facing challenges in subjective environmental evaluation [20]. To address this issue, evaluating thermal environments based on objective parameters (e.g. skin temperature) has been found reliable. Skin temperature has been widely recognized as a thermal comfort indicator [7,21,22]. Thus, investigating fundamental characteristics of skin temperature responses based on thermal balance has been a research topic [23]. Thermoregulation models have been developed as effective tools to predict overall [24] and local skin temperatures [25,26]. The models can be further used for heatstroke prediction [27], predicting physiological status [28], predicting core temperature [29], etc.

1.2 Literature review of thermoregulation models of the elderly

Thermoregulation models are based on physiology, thermodynamics and thermobalance theory to predict both skin and core temperatures [30]. Thermoregulation models consist of two systems: the passive system and the active system [31,32]. The passive system of the human body includes a geometric abstraction of the human body and an abstraction of the thermophysical interaction between the skin and the thermal environments. In the human body, heat is produced by metabolic and muscle activity. Then heat is transferred from the interior to the skin by thermal conduction and blood convection. The heat dissipation to ambient environments is through convection, radiation, respiration, and perspiration. In comparison, the function of the active system is to keep the body's core temperature within a narrow range. This is accomplished by the autonomic nervous system's control of thermoregulatory activities, including sweating, shivering, vasoconstriction, and vasodilation. The activities are controlled by both active coefficients (to determine the intensity of the thermoregulatory activities) and set point temperatures (to trigger the thermoregulatory activities and determine intensity) [33]. Most of the prevailing thermoregulation models are established for non-elderly adults (aged < 60) and further incorporate reduced functions in thermoregulation activities and physiological changes in elderly people [30]. The existing thermoregulation models for the elderly can be divided into three categories according to the number of segments and nodes: one-segment single-node models, one-segment multi-node models, and multi-segment multi-node models. Examples of segmentations and node distributions of these models are shown in Fig. 1.

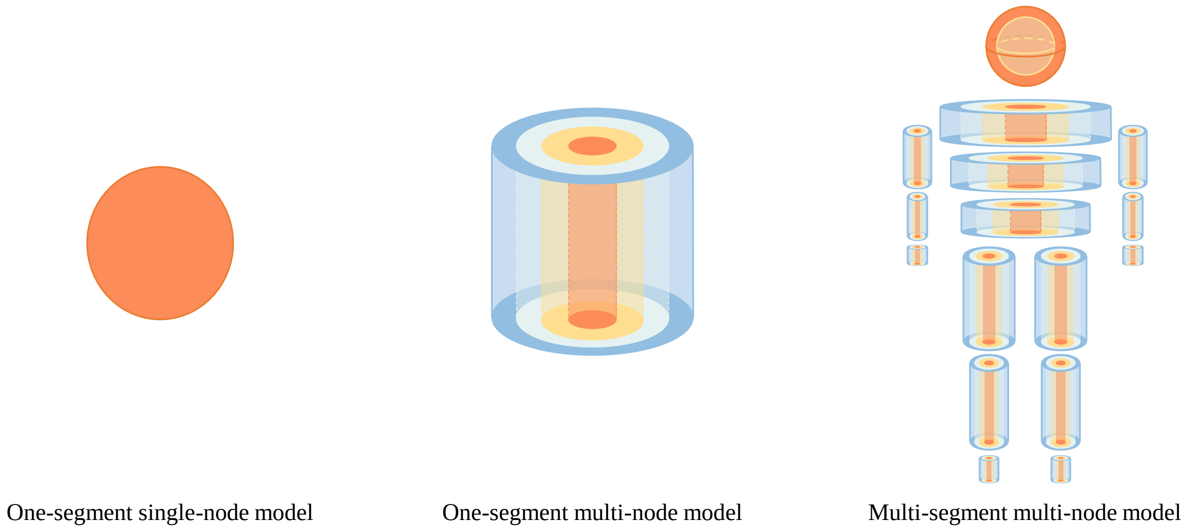

Fig. 1. Diagram of the segmentation and layering of thermoregulation models.

1.2.1 One-segment single-node thermoregulation model

A representation of the one-segment single-node model is Fanger's PMV-PPD (predicted mean vote and predicted percentage of dissatisfied) index [34]. The PMV value is calculated using the thermal load multiplied by a thermal sensation transmission coefficient [35,36], where skin temperature is set to be linearly related to the difference between the metabolic rate (M, W/m^2) and the external work (W, W/m^2), as shown in Eq. (1).

$$T_s = 35.7 - 0.028(M - W) \tag{1}$$

Where T_s is skin temperature, ˚C. For example, when the metabolic rate is 1.1 met (1 met = 58.15 W/m^2) and the external work is 0 during office activities, the corresponding skin temperature is fixed at 34.1˚C regardless of environmental parameters. However, studies have found that skin temperature is related to ambient air temperatures [7,37] and air speeds [38]. Additionally, its active system is quite straightforward. Regular heat loss through sweating is linearly proportional to the metabolic rate regardless of actual skin temperature and no other regulative activity is controlled. Thus, the PMV-PPD index cannot reflect the influences of thermal environments and active parameters on skin temperature. Moreover, the index is primarily effective under steady-state and uniform conditions [39]. In this regard, it is challenging to assess thermal comfort using the PMV-PPD index for the elderly.

1.2.2 One-segment multi-node thermoregulation model

One-segment multi-node thermoregulation models simplify the human body into a multi-layer cylinder. One of the most well-known models is Gagge’s two-node model [40,41], which treats the human body as a double-layer cylinder composed of core and skin layers [40,42]. Based on Gagge’s two-node model, Ji *et al.* [43] proposed an improved thermoregulation model for the elderly group considering the age-related changes in the active system. The age-related attenuation coefficients and the threshold values (set points) were proposed to reflect the deterioration in thermoregulatory functions of the elderly.

Another optimized individualized one-segment three-node thermoregulation model [44] was established based on an existing three-node model [45] with layers of core, bare skin, and clothed skin. Individualization of the model was achieved by integrating the effects of age, gender, height, and weight on passive parameters. The passive parameters include body surface area, body fat percentage, fat thickness, basal metabolic rate, etc. The active system activities were modified by skin surface area. With a similar aim, the model was further modified by dividing the body into core, muscle, fat (subcutaneous), epidermis, and dermis with their respective thermal properties [46].

From the above research, it can be seen that age influences the basal metabolic rate, body density, body fat percentage, cardiac output, vascular activity, etc. The previous studies to modify one-segment multi-node models for the elderly mainly focus on either the active system [43] or the passive system [44,46]. The first type overlooked the effects of physical parameters including gender, fat percentage, height, weight, etc., while the second type ignored decreased thermoregulatory activities among the elderly. However, few studies have been able to draw on any comprehensive research into a combined consideration of the passive and the active systems.

1.2.3 Multi-segment multi-node thermoregulation model

In multi-segment models, the passive system is divided into several body segments. Each segment is a concentric cylinder or sphere. The prevailing human thermoregulation models are the Stolwijk model [47], the Fiala model [48–50], the Tanabe model [51], the Huizenga model [52], etc. The models are established using data from young adults. These models have diverse body segmentation and different control equations for active systems. Based on the existing thermoregulatory models for the young, the models for the elderly are usually modified with some age-related changes. The passive parameters mainly include body weight, height, body surface area, fat percentage or thickness, metabolic rate, cardiac output, skin blood flow, segment length and radius, heart rate, and muscle thickness [53–59]. As for the active system, the parameters were optimized in a variety of ways. Novieto [53] modified the sweating, shivering, and vasomotor signal coefficients with a genetic algorithm. Takahashi *et al.* [54] considered age effects on brown adipose tissue thermal production, sweating, cardiac output, skin blood flow, and shivering by multiplying respective aging factors. In comparison, Rida *et al.* [55] and Coccarelli *et al.* [59] focused on the threshold temperatures for the active system, including maximum vasodilation, maximum vasoconstriction, and the sweating threshold.

The multi-segment multi-node models are capable of predicting local skin temperatures. However, the utilization of multi-segment multi-node models in estimating the thermal responses of elderly individuals requires more fundamental data to improve the accuracy. For example, detailed blood flow measurements are required for model input, including artery, vein, superficial vein, and arteriovenous anastomosis blood flow for each body part [54,55].

1.3 Aims and objectives

In the review of the existing thermoregulation models for the elderly, it has been observed that the PMV-PPD method is easy to use but may have certain limitations when estimating the dynamic thermal responses. Multi-segment multi-node thermoregulation models have more detailed segmentation; however, modifying these models requires a large quantity of fundamental data about the elderly. In comparison, one-segment multi-node models have many advantages over the other two types of models, including simpler model configuration, fewer computational procedures, fewer input parameters, and the ability to explain the heat transfer characteristics inside the human body. Thus, this study aims to develop and validate a new one-segment multi-node thermoregulation model for the elderly. The novelty of the model is a comprehensive consideration of the passive and active parameters and an introduction to a more explainable optimization method of the active parameters. The objectives are: 1) To demonstrate demographic representation and define the applicable population of the proposed model; 2) To use sensitivity analysis to quantify the influence of passive parameters and adjust those values using measurement or literature data; 3) To optimize the active system by resetting body temperature set points and optimizing active parameters.

2. Modeling theory and data acquisition

An existing model verified with groups of young Chinese (average age 24 years) [60] was used as the base model. This model [60] was established by simplifying the human body into a four-layer cylinder, representing the core, muscle, fat and skin. A central blood node exchanges heat with every layer. The passive system followed the thermal balance theory in the forms of heat conduction, convection, radiation and evaporation. The active system determines signal inputs for the core and skin; thus the signals can be used as the inputs of each layer to control blood flow, sweating and shivering.

2.1 Theory and configuration of the base model

2.1.1 Thermal balance theory

As the basis of the thermal balance theory of the human body, the basic energy equation (Eq. 2) followed the classic Pennes bio-heat equation [61]:

$$\lambda_i\left(\frac{\partial^2 T_i}{\partial r^2}+\frac{1}{r_i}\frac{\partial T_i}{\partial r}\right)+q_i+c_{\mathrm{bl}}\rho_{\mathrm{bl}}w_{\mathrm{bl}}(T_{\mathrm{bl}}-T_i)=\rho_i c_i\frac{\partial T_i}{\partial \tau} \tag{2}$$

Where the subscripts $_{\mathrm{bl}}$ and $_i$ represent blood and the *i*th layer of body tissue, respectively. λ_i is the thermal conductivity coefficient at the *i*th layer, W/(m·k); T_i is the temperature of the body tissue at the *i*th layer, ˚C; r_i is the radius from the *i*th layer to body center, m; $\lambda_i\left(\frac{\partial^2 T_i}{\partial r^2}+\frac{1}{r_i}\frac{\partial T_i}{\partial r}\right)$

shows thermal conduction along the radius direction, W/m^3; q_i is thermal production of metabolism of the ith layer, W/m^3; c_{bl} and c_i are the specific heat of blood and the ith layer, respectively, J/(kg·k); ρ_{bl} and ρ_i are the density of blood and the ith layer, respectively, kg/m^3; w_{bl} is the blood perfusion rate per cubic meter, m^3/(s·m^3); T_{bl} is the temperature of blood, ˚C; $c_{\mathrm{bl}}\rho_{\mathrm{bl}}w_{\mathrm{bl}}(T_{\mathrm{bl}} - T_i)$ is the heat convective exchange by blood circulation between the central blood and the ith layer, W/m^3; τ is time, s; and $\rho_i c_i \frac{\partial T_i}{\partial \tau}$ is heat storage of the ith layer with time, W/m^3.

2.1.2 Model configuration

In the physical model of the human body, the temperature distribution is the same in the vertical radius direction and the heat transfer process occurs along the radius direction. The structure of the passive system is shown in Fig. 2, which is adapted from the base model [60]. The human body was abstracted into one cylinder (one segment) and four lumped layers: core, muscle, fat and skin. The central blood pool performs heat convection exchange with four nodes through arterial and vein blood flow. Between the adjacent two layers, heat is transferred by heat conduction. Metabolic heat is produced in three ways: basal metabolism, activity thermogenesis and shivering thermogenesis.

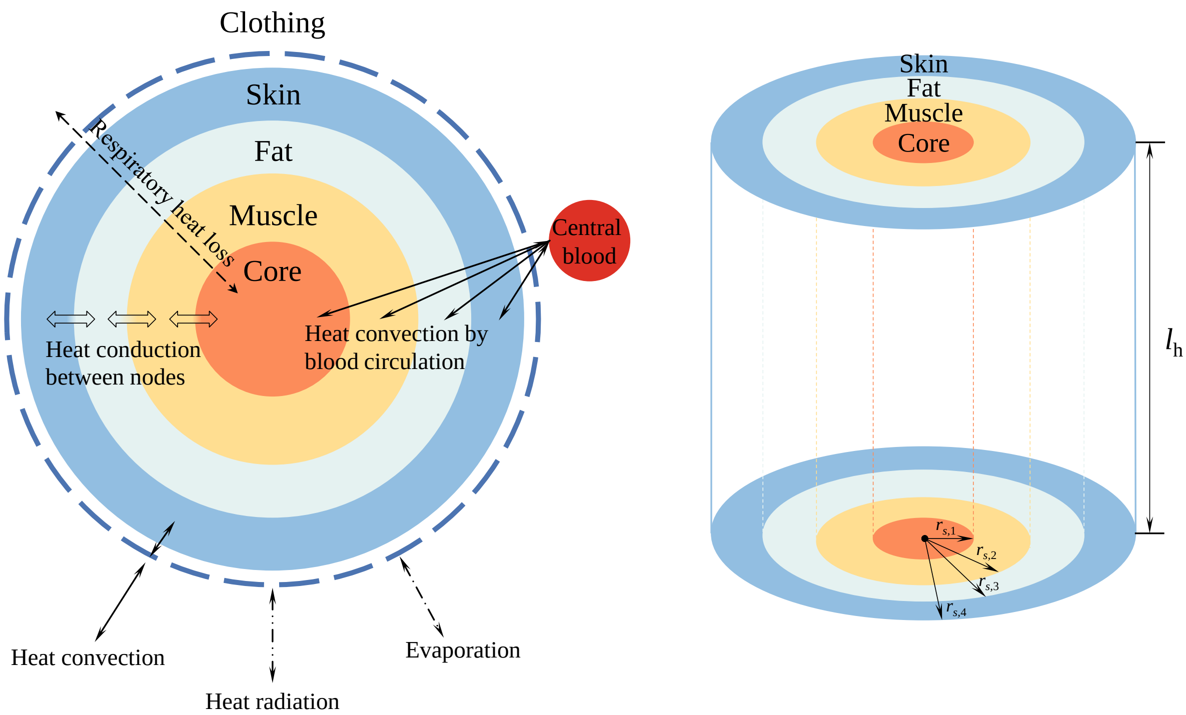

Fig. 2. Model configuration and thermal exchange processes of the model (adapted from [60]). l_h: Height of the model, m; $r_{s,i}$: Radius of the outer boundary of the ith layer, m.

The dimension of the model is determined by Eqs. (3) and (4).

$$l_h = A^2/4\pi \sum_{i=1}^{4} V_i \tag{3}$$

$$r_{s,i} = \sqrt{\sum_{i=1}^{4} V_i\,/\pi l_h} \tag{4}$$

Where l_h is the height of the model, m; and $r_{s,i}$ is the radius of the outer boundary of the ith layer, m; A is the body surface area of the human body, m^2; V_i is the volume of the ith layer, m^3.

The active system activities are controlled with Eqs. (5)–(14), which are associated with input signals. As shown in Table 1, input signals of the core and skin layers Err_c and Err_s (°C) are closely related to core and skin set points $T_{set,c}$ and $T_{set,s}$ (°C), which are the temperatures of the core and skin layers at the neutral state. From the control expressions, it can be seen that the active parameters include C_{dl}, S_{dl}, C_{st}, S_{st}, C_{sw} and C_{sw}. The symbols C and S mean coefficients of the core layer and the skin layer, respectively. The subscripts $_{dl}$, $_{st}$ and $_{sw}$ mean vasodilation, vasoconstriction and sweating activity, respectively. The modification of set points and active parameters of the elderly are shown in Section 4.

Table 1. The mathematical expression of the control mechanisms of active system activities.

Terms in the active system activities	**Mathematical expression**	**Eq. No.**
The input signal of the core layer receptor when $F_c > 0$	$Err_c = T_c - T_{set,c}$	(5)
The input signal of the core layer when $F_c < 0$	Male: $Err_c = T_c - T_{set,c}$ Female: $Err_c = T_c - T_{set,c} + 1800 \times F_c$	(6) (7)
The input signal of the skin layer receptor when $F_s > 0$	$Err_s = T_s - T_{set,s}$	(8)
The input signal of the skin layer when $F_s < 0$	Male: $Err_s = T_s - T_{set,s}$	(9)
	Female: $Err_s = T_s - T_{set,s} + 1800 \times F_s$	(10)
Skin blood flow	$BF_s = \frac{BFB_s + DL}{1 + ST} \times 2^{Err_s/10}$	(11)
	$DL = \max\{0, C_{dl}Err_c + S_{dl}Err_s\}$	(12)
	$ST = \max\{0, -C_{st}Err_c - S_{st}Err_s\}$	(13)
Sweating	$E_{sw} = (C_{sw}Err_c + S_{sw}Err_s)2^{Err_s/10}/A$	(14)

Note: F_c is the temperature change rate of the core layer, ˚C/s; F_s is the temperature change rate of the skin layer, ˚C/s; Err_c is the input signal of the core layer, ˚C; Err_s is the input signal of the skin layer, ˚C; T_c and $T_{set,c}$ are the core layer temperature and set point, respectively, ˚C; T_s and $T_{set,s}$ are the skin layer temperature and set point, respectively, ˚C; BF_s is the blood flow rate of the skin layer, L/h; BFB_s is basal blood flow at the neutral thermal condition with 11.89 L/h for the young group. C_{dl} and S_{dl} are the vasodilation coefficients for the core and skin layer, respectively, L/(h·˚C). C_{st} and S_{st} are the vasoconstriction coefficients for the core and skin layer, respectively, 1/˚C. C_{sw} and S_{sw} are the sweating coefficients for the core and skin layer, respectively, W/˚C·m^2.

2.1.3 Numerical discretization

This study follows the same numerical discretization method used in the basic model and is further explained and illustrated in detail. As the numerical distribution of temperature in the actual heat transfer process is continuous, the space and time of the thermoregulation models are discretized using the finite difference method. This model is based on differential equations and is calculated with discrete nodes at spacing Δ*r*=0.002 m along the radius direction and at time interval Δ*t*=1 s. Such values satisfy the stability of the numerical solution and reduce the computation time. On this basis, the discrete equations are established for each internal and boundary node combining the Taylor series expansion method. Under steady-state conditions, the energy equation is Eq. (15) :

$$\lambda_j\left(\frac{\partial^2 T_j}{\partial r_j^2}+\frac{1}{r_j}\frac{\partial T_j}{\partial r_j}\right)+q_j+c_{\mathrm{bl}}\rho_{\mathrm{bl}}w_{\mathrm{bl}}\left(T_{\mathrm{bl}}-T_j\right)=0 \tag{15}$$

Where subscript j represents the jth node; r_j is the distance from the jth node to the center of the model, m; λ_j is the thermal conductivity coefficient at the ith node, W/m•K; T_j is the temperature of the body tissue at the jth node, ˚C.

The internal nodal heat transfer energy equation is expressed in Eqs. (16) and (17):

$$T_j=\frac{\Delta r^2}{2\lambda_j}(\lambda_j\frac{T_{j+1}-T_{j-1}}{2r_j\Delta r}+\lambda_j\frac{T_{j+1}-T_{j-1}}{\Delta r^2}+q_j) \tag{16}$$

$$T_{\tau,j}=\lambda_j\Delta t\frac{T_{\tau-1,j+1}-T_{\tau-1,j-1}}{2r_j\Delta r\rho_j c_j}+\lambda_j\Delta t\frac{T_{\tau-1,j+1}-T_{\tau-1,j-1}}{\Delta r^2\rho_j c_j}+q_{\tau-1,j}\frac{\Delta t}{\mathrm{c}c_j}+(1-\frac{2\lambda_j\Delta t}{\Delta r^2\rho_j c_j})T_{\tau-1,j} \tag{17}$$

Where $T_{\tau,j}$ is the temperature of the jth node at the time τ, ˚C; Δr is the spatial discrete spacing, 0.002 m; q_j is thermal production of metabolism of the jth node, W/m^3; subscripts $_{j+1}$ and $_{j-1}$ are the next and last inner node; ρ_j is the density of the jth node, kg/m^3; c_j is the specific heat of the jth node, J/(kg·k); subscript $_{\tau-1}$ is the last time, s.

For the three boundary layers (core-muscle layer, muscle-fat layer and fat-skin layer) and at the poles, the discretization of the boundary layers for steady and transient processes are shown in Eqs. (18)–(19):

$$T_j=(\frac{\lambda_{j-1}}{\Delta r^2}T_{j-1}-\frac{\lambda_{j-1}}{2r_j\Delta r}T_{j-1}+\frac{\lambda_{j+1}}{\Delta r^2}T_{j+1}+\frac{\lambda_{j+1}}{2r_j\Delta r}T_{j+1}+\frac{q_{j-1}+q_{j+1}}{2})/(\frac{\lambda_{j-1}}{\Delta r^2}-\frac{\lambda_{j-1}}{2r_j\Delta r}+\frac{\lambda_{j+1}}{\Delta r^2}+\frac{\lambda_{j+1}}{2r_j\Delta r}) \tag{18}$$

$$\frac{\partial T_j}{\partial r}|_{r=0}=C_{\mathrm{res}}+E_{\mathrm{res}} \tag{19}$$

Where q_{j-1} and q_{j+1} are the intensity of the internal heat source at the upstream node and the downstream node of the boundary node, respectively, W/m^3; λ_{j-1} and λ_{j+1} denote the thermal conductivity of the upstream node and the downstream node, respectively, W/m·K. C_{res} and E_{res} are the convective and evaporative heat dissipation, W/m^2.

2.2 Data acquisition from the elderly for model optimization

To establish and modify the model, measured data needed to be collected from the Chinese elderly. The data acquisition was done in a well-controlled climate chamber. The characteristics of the climate chamber and the adjacent preparation room have been described in detail in existing studies [62–64]. To properly activate the thermal regulatory responses of the human body and collect a variety of skin temperatures under transient conditions, warm-neutral-warm temperature step change experiments were designed. The air temperature was determined to be 25˚C with 50% relative humidity (RH) as the neutral environment [65], while the warmer temperatures were 28, 30, 32 and 34˚C with 60% RH. Air speed was kept at ≤ 0.1 m/s. Accordingly, there were three stages in the experimental sessions as shown in Fig. 3. Stage 1 was designed as a warm condition with one of the four levels (28, 30, 32, or 34˚C) for 30 minutes. Then stage 2 started when the subjects moved back to the preparation room (25˚C) and lasted for 60 minutes. Then, elderly subjects moved to the climate chamber again for another 30 minutes with an air temperature in stage 3 the same as that in stage 1.

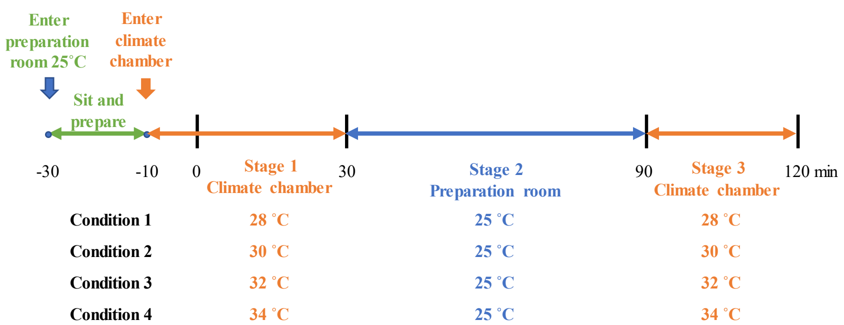

Fig. 3. Experimental protocols.

Ten local skin temperatures were continuously measured throughout the whole experimental process at 30-second intervals. The instruments used for measuring skin temperatures were skin temperature sensors (Type: TMC6-HE) with a measuring range of −40–100˚C and an accuracy of ±0.21˚C. The mean skin temperatures were calculated by weighting the following ten sites: head (0.06), chest (0.12), abdomen (0.12), back (0.12), upper arm (0.08), lower arm (0.06), hand (0.05), upper leg (0.19), calf (0.13) and foot (0.07) [66].

2.3 Subjects and demographic representation

There were 24 elderly participants who were within the normal range (18.5–30.0 kg/m^2) [67] of body mass index (BMI). The participants were between 60 and 74 years old. The ethics approval number is CCNU-IRB-2019-002. Written informed consent was obtained from every participant. Every participant experienced all the experimental protocols. A key element of the thermoregulation model is its demographic representation which confines its applicable population and corresponding anthropometric characteristics. As the scope of the present model applied to the Chinese elderly, the demographic representation was verified by comparing the demographic (age) and physical (weight, height, fat percentage and BMI) parameters of the experimental subjects to those from the census. Since age is not normally distributed in the elderly population (60+ years), the standard age of this study was defined as the 50th percentile (median) of the elderly population. According to the 2022 Chinese census data [68] and cumulative distribution by age group shown in Fig. 4, 66 years was the median age. The results in Table 2 showed that the relative differences between subjects' data and national data were all lower than 4%. The good fit between the census data and the data of the modelling subjects allows the prediction model to be representative of the Chinese elderly population, maximizing its applicability and having lower prediction bias due to group differences.

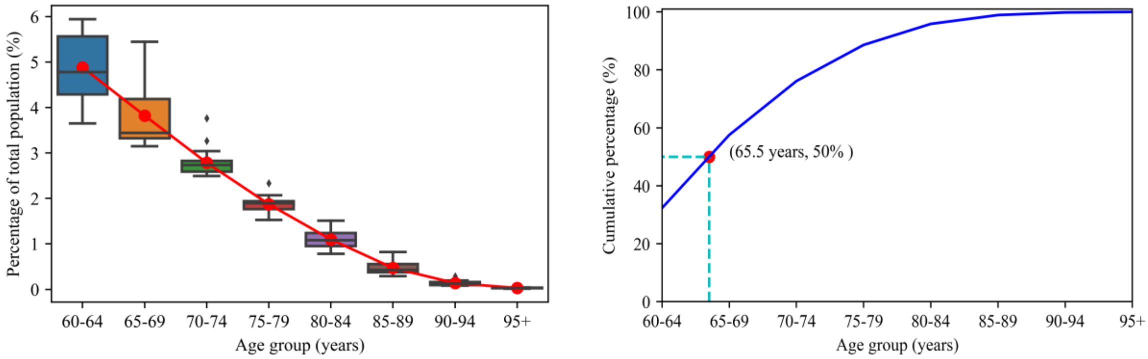

(a) Distribution of people over 60 years old in China in 2022 [68]

(b) Cumulative distribution by age group

Fig. 4. Age distribution of the census.

Table 2. Comparison between subjects' anthropometric data in the present study and national census data in 2022 [69].

Data source	**Gender**	**Age (year)**	**Weight (kg)**	**Height (m)**	**Body mass index (kg/m^2)**	**Fat percentage (%)**
Subjects' data	Male	67.3±1.4	66.1±2.9	1.63±0.02	24.8±1.0	23.6±1.0
	Female	66.3±1.0	58.1±2.3	1.51±0.02	24.2±0.7	34.3±1.2
National data [69]	Male	66	68	1.65	25.0	23.3
	Female	66	60	1.54	25.1	33.0

Note: The subjects' data are presented with mean ± standard deviation. The national data are presented with the median age and average weight, height, body mass index and fat percentage values for the median age.

3. Optimization of the passive system

Due to the variation in age-related decay of the thermoregulation abilities of the elderly, the passive system was optimized by sensitivity analysis and the corresponding parameters were adjusted by measurement or literature data.

3.1 Sensitivity analysis of passive parameters

All the passive parameters of the base model are divided into two types. The first type was initially adjusted according to the physical data of elderly subjects. Thus, height, weight, gender and clothing insulation were directly changed in the model. The second type cannot be directly measured so the quantified effects including basal metabolic rate, body surface area (BSA), fat percentage, basal skin blood flow and cardiac output are unknown. As a result, these parameters need further sensitivity analysis to evaluate their influence on skin and core temperatures. In the present study, sensitivity analysis adopted a local approach belonging to the one-factor-at-a-time method [70]. Thus, only one variable is altered while all the others are stable. In Table 3, the values indicate changes compared to the base case (Chinese young adults) [60] that were determined from existing literature quantifying age-related physiological changes. Relative changes of “0” mean no change from the base model. The relative changes in BSA were determined by the results using different calculation methods in the references [54,58,60].

Table 3. Input parameters and values for sensitivity analysis.

Parameter	**Unit**	**Base case value**	**Relative changes from base case**	**Reference**
Basal metabolic rate	W/m^2	44	0, −10%, −20%, −30%	[43]
BSA	m^2	Male: 0.0057×H+0.0121×W+0.0882 Female: 0.0073×H+0.0127×W-0.2106	−15%, −10%, −5%, 0, +5%, +10%, +15%	[54,58,60]
Fat percentage	%	34.3 for females and 23.6 for males	0, +10%, +20%, +30%	[53,69]
Basal skin blood flow	L/h	11.89	0, −10%, −20%, −30%, −40%, −50%	[71]
Cardiac output	L/h	285	0, −10%, −20%, −30%, −40%	[58]

Note: BSA, body surface area; H, height (m); W, weight (m).

A thermoneutral condition and a warm condition were selected as the environmental conditions for sensitivity analysis: indoor operative temperature of 26˚C or 34˚C, RH of 60%, air speed of 0.1 m/s, clothing insulation of typical summer clothing 0.5 clo. The simulation time was 1 hour and the results for the 60th minute were analyzed and shown in the following section.

3.2 Sensitivity analysis results and interpretation

Sensitivity analysis results of mean skin temperatures and core temperatures are shown in Fig. 5. It can be seen that for both males and females, higher body fat percentages can result in lower mean skin temperatures. This result is consistent with the existing finding that higher fat layer thickness can reduce heat conduction from inside to outside the body. This is also the reason that elderly people have lower skin temperatures than the young group. The lower cardiac output can result in lower thermal exchange due to blood circulation. Similarly, as a branch of blood output from the heart, skin blood flow has the same way of influencing mean skin temperature by reducing the heat exchange between the skin layer and ambient environment.

In comparison, core temperatures rose with body fat percentage, as a result of less heat dissipated from and more heat retained within the human body. For the reduced cardiac output and skin blood flow, less heat can be circulated from the central blood to each layer and from the skin layer to the surroundings. From the results above it can be seen that all the analyzed parameters have apparent influences on the physiological responses of the elderly, although the influence of body surface area is not as great as those of the other parameters. This identifies the importance of selecting accurate parameters for the elderly with the values needing to be carefully determined to represent the age-related physiological changes of the elderly.

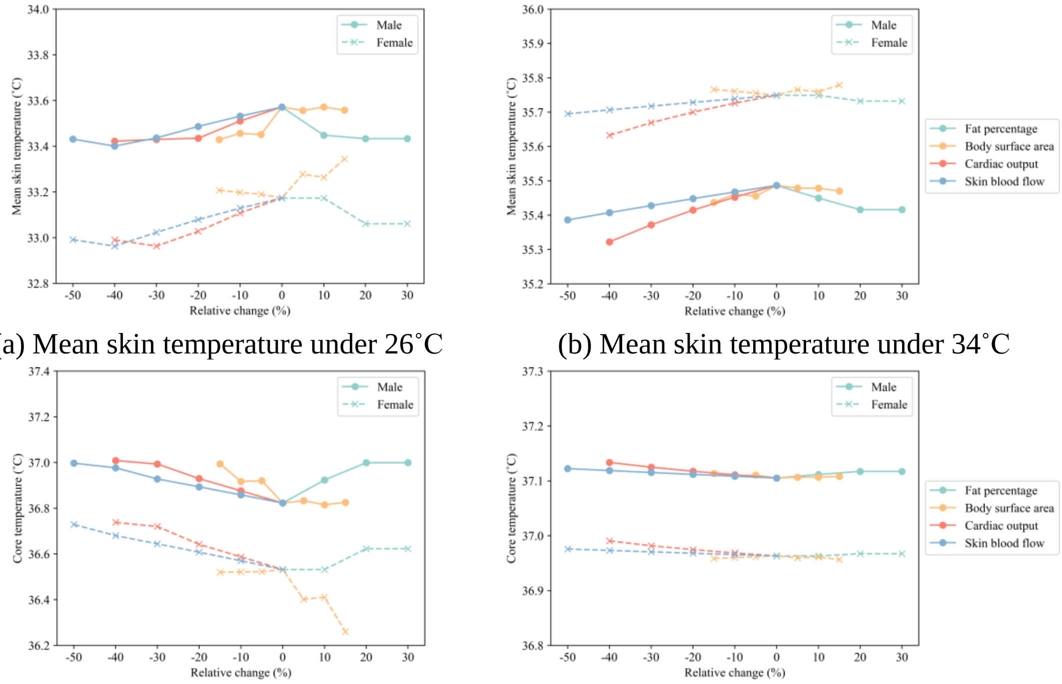

(a) Mean skin temperature under 26˚C (b) Mean skin temperature under 34˚C

(c) Core temperature under 26˚C (d) Core temperature under 34˚C

Fig. 5. Sensitivity analysis results.

3.3 Optimized passive system parameters

As a consequence of the sensitivity analysis's findings, the following values were adjusted for Chinese elderly people. The values were directly measured or obtained from published research.

- Body weight of 66 kg for males and 58 kg for females.
- Body height of 1.63 m for males and 1.51 m for females.
- Body fat percentage of 23.6% for males and 34.3% for females according to the

measurement statistics for the subjects.

- BSA was obtained from the equations customized for the Chinese elderly [58].
- A 20% reduced metabolic rate from [53,58,72] with 0.8 met (1 met = 58.15 W/m^2) when sitting.
- Skin blood flow reduced to 8.9 L/h, 25% lower than for young adults [54].
- Cardiac output reduced to 223.2 L/h for Chinese elderly [58].

4. Optimization of the active system

After changing all the passive systems in the model, the active system was then optimized. The corresponding set points and active parameters were modified as stated above.

4.1 Modification of body temperature set points

The body temperature set point is a key element in the active system because the error signals were all calculated based on the set points, as shown in Section 2.1.2. When the body temperature is at the set point temperature, the thermal sensation is neutral and the body has no significant active system responses, i.e. no significant sweating or shivering activities. Meanwhile, the cardiac output and skin blood flow remain at basal blood flow levels. Under this condition, the body’s heat- and cold-sensitive neurons are in a state of equilibrium. The set points for male and female elderly were separately calculated in the present model. Linear regressions of thermal sensation vote against air temperature were performed to obtain the neutral air temperatures at thermal sensation votes equal to 0. The obtained neutral temperatures were 26.7˚C for males and 26.5˚C for females. The neutral temperatures were input into the model as environmental settings. Meanwhile, sensible sweating and shivering were set to zero. After calculating the temperature of each layer for 3,600 seconds, the set points in layers were obtained, as shown in Table 4. Compared with the young group, the elderly have lower neutral skin temperature and lower neutral core temperature; as found in previous studies [73,74].

Table 4. Set points (˚C) of layers of the elderly model and the base model.

Age group	**Gender**	**Core**	**Muscle**	**Fat**	**Skin**	**Central blood**
Elderly	Male	36.6	36.5	36.0	34.2	36.4
	Female	36.4	36.3	35.7	33.6	36.2
Young [60]	Male	36.9	36.5	35.3	34.2	36.7
	Female	36.7	36.4	35.1	33.8	36.5

4.2 Optimization of active parameters

Under neutral and warm environments, the main thermoregulatory activities include vasodilation, vasoconstriction and sweating. In this way, the parameters to be optimized include C_{dl}, S_{dl}, C_{st}, S_{st}, C_{sw} and C_{sw}, as introduced in Section 2.1.2.

4.2.1 Target function

An optimal combination of active parameters enables the model to perform with high prediction accuracy. As a result, the target function should first be determined to evaluate model performance. Root mean square error (RMSE) has been a frequently used evaluation method for thermoregulation models [33,54,75,76]. RMSE quantifies model performance using the differences between predicted and measured values. In this study, the error was evaluated using Eqs. (20) and (21).

$$RMSE = \sqrt{\sum_{k=1}^{120} (T_{sk,k} - \hat{T}_{sk,k})^2 / 120} \tag{20}$$

$$ARMSE_{gender} = \frac{\sum_{n=1}^{4} RMSE_{n,gender}}{4} \tag{21}$$

where $\hat{T}_{sk,k}$ is the model output mean skin temperature at the *k*th minute, ˚C; $T_{sk,k}$ is the measured mean skin temperature at the *k*th minute, ˚C; RMSE is the mean squared error of the model per condition, ˚C^2; $RMSE_{n,gender}$ is the RMSE of the *n*th condition of males or females, ˚C^2; $ARMSE_{gender}$ (average root mean squared error) is the target function to determine model performance, i.e. the mean of RMSE for the four conditions (n = 1–4) for males or females, ˚C^2.

4.2.2 Selection of the optimization algorithm

This study selected a hyperparametric optimization search method. Among the methods used in deep learning, TPE (Tree-structured Parzen Estimator) is a hyperparameter tuning method based on Bayesian optimization. The core idea of TPE is to use *a priori* knowledge to gradually narrow down the hyperparameter search and finally get the optimal combination of hyperparameters. The method has higher efficiency and accuracy compared with traditional grid search and random search methods [77].

4.2.3 Results and interpretation

The change ranges of the active parameters were first defined. For each parameter, ranges between −50% and +50% of the original values were determined and the TPE search was conducted in 1% steps. The model was optimized for 100 trials and the results are shown in Fig. 6. The TPE algorithm can adaptively adjust the exploration range to achieve a stabilized ARMSE after 40 iterations. The accuracy can achieve the best performance within 75 iterations. The calculated ARMSE is 0.1˚C for females and 0.4˚C for males.

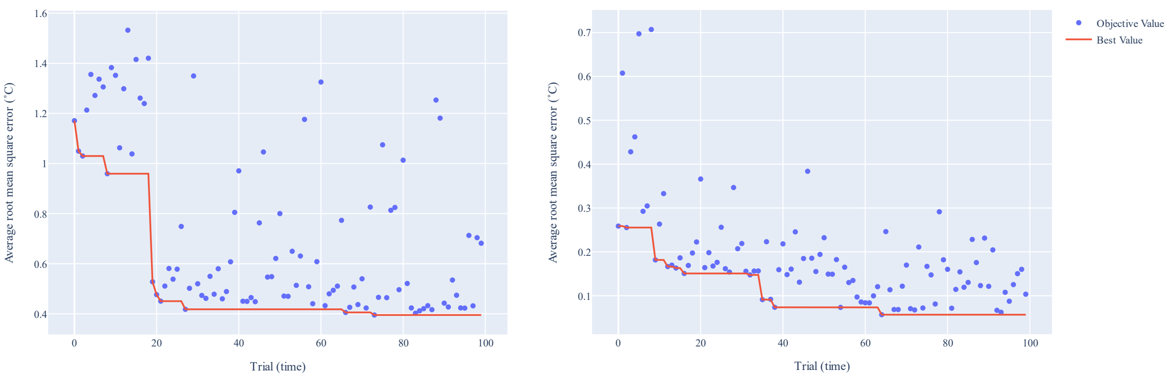

(a) Male elderly (b) Female elderly

Fig. 6. Average root mean squared error results of the tested 100 rounds.

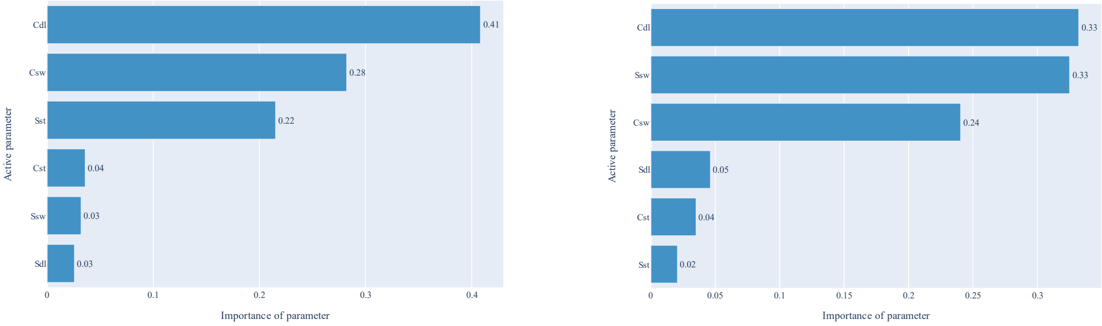

(a) Male elderly (b) Female elderly

Fig. 7. Parameter importance on the results of average root mean squared error.

Fig. 7 further interprets the relative importance of the passive parameters on the ARMSE results. For both males and females, the core vasodilation coefficients and the core sweat coefficients have been the most influential factors. In other words, the changes in these parameters have greater influence on the model prediction accuracy than other parameters. Moreover, the model performance for males is also influenced by skin vasoconstriction coefficients. This is because elderly males have higher neutral skin temperature (34.2˚C) than females (33.6˚C). Under the same thermal condition, vasoconstriction is more easily triggered in males. The optimum combination of the active parameters is shown in Table 5.

Table 5. Optimum active parameters.

Age group	**Gender**	C_{sw}	S_{sw}	C_{dl}	S_{dl}	C_{st}	S_{st}
The elderly	Male	168.17	7.56	34.67	4.13	0.63	0.93
	Female	85.85	3.29	37.14	2.70	0.49	0.92
The young [60]	Male	117.60	10.80	61.90	3.97	0.63	0.63
	Female	58.80	5.40	61.90	3.97	0.63	0.63

Note: C_{sw}, the sweating coefficient for the core layer, W/ ˚C·m^2; S_{sw}, the sweating coefficient for the skin layer, W/ ˚C·m^2; C_{dl}, the vasodilation coefficient for the core layer, L/(h·˚C); S_{dl}, the vasodilation coefficient for the skin layer, L/(h·˚C); C_{st}, the vasoconstriction coefficient for the core layer, 1/˚C; S_{st}, the vasoconstriction coefficient for the skin layer, 1/˚C.

5. Model validation

5.1 Validation data

The model was validated with a set of published data [63] originating from thermal comfort experiments in a climate chamber under temperature ramps. Sixteen healthy gender-balanced elderly people participated in the experiments and experienced both thermal conditions. The average physical data for this group of elderly people were: age 64 years, weight 61.4 kg, height 1.6 m, BMI 23.9 kg/m^2 and body fat percentage 27.3%. The subjects were dressed in summer apparel with an average thermal resistance of 0.55 clo. A temperature ramp-up condition (from 18 to 34˚C within 150 min) and a temperature ramp-down condition (from 34 to 18˚C within 150 min) were tested. During the studies, relative humidity was around 55% and nearly no wind (roughly 0.05 m/s). Measured mean skin temperatures were calculated from the four local skin temperatures with corresponding weights: chest 0.3, upper arm 0.3, thigh 0.2 and calf 0.2. Before the test started, the participants rested in the preparation room for half an hour to evaporate all sweat and eliminate the influences of previous thermal experiences. As shown in the study [63], the room setting temperature rose or decreased by 2˚C every 15 minutes. Accordingly, the above-mentioned parameters and the recorded air temperature settings were input into the developed thermoregulation model. In this way, the simulation of the temperature ramps was achieved by inputting a series of temperature conditions and periods.

5.2 Validation process and model performance

The validation of the model was achieved by inputting thermal conditions and periods in Section 5.1 of the temperature ramps into the model. In this way, the thermal conditions were simulated. The other parameters were the same as the validation experiment scenarios. The metabolic rate was set as 0.8 met and the clothing insulation was set as 0.55 clo. Relative humidity was kept at 55%. In this way, the model can simulate and output a series of skin temperature results with time. By changing the temperature change direction and preset genders, the model output can also demonstrate gender differences under different thermal conditions. The predicted skin temperatures were compared with the actual measured data and the original model in Fig. 8. Fig. 8 (a) and (b) represent the results of the ramp-down thermal condition (34–18˚C) for males and females, respectively. Results show the optimized model's prediction results were closer to the measured data with less overall bias than the original model prediction, indicating a better prediction performance of the optimized model in this study. Similar results can also be found in Fig. 8 (c) and (d) under the ramp-up thermal condition (18–34˚C) for males and females, respectively. The optimized model prediction results were also closer to the measured data and more prediction data fell into the 95% confidence interval. As a result, Fig. 8 shows the higher performance of the optimized model for the elderly than the original model for the young. To quantify the model performance and compare it with other thermoregulation models for the elderly, RMSE was calculated to evaluate the deviation between the actual and predicted mean skin temperature. The calculated RMSE ranged from 0.10 to 0.35˚C under the four scenarios, which is a range lower than other models for the elderly, including the 0.58–0.83˚C of the joint system thermoregulation model [54] and 0.2–0.4˚C of a modified Stolwijk model [76]. The results indicate a good prediction ability for the developed thermoregulation model.

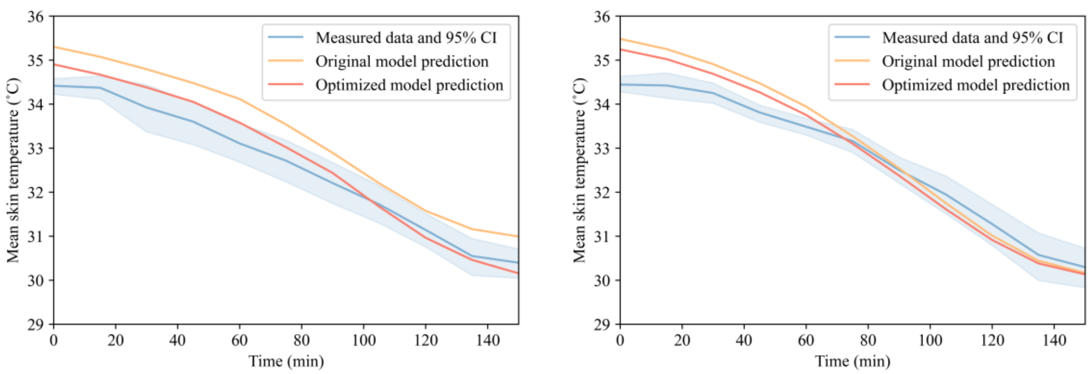

(a) Ramp down, male

(b) Ramp down, female

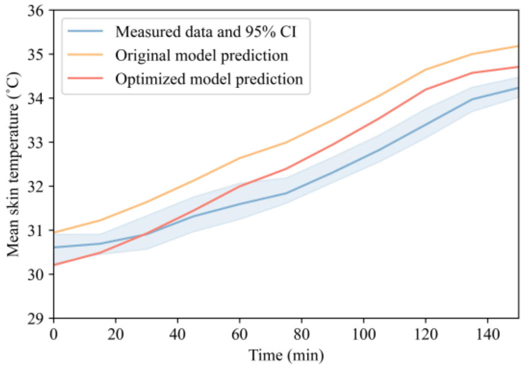

(c) Ramp up, male

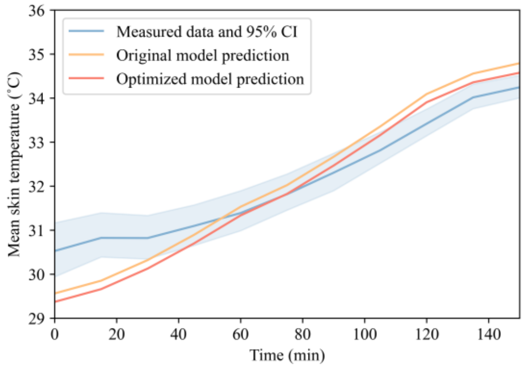

(d) Ramp up, female

Fig. 8. Model performance of ramp down and up conditions for elderly males and females. CI: Confidence interval.

6. Discussion

6.1 Advantage and improvement over the existing models

The proposed model's applicability for the elderly in China was demonstrated and it effectively predicted mean skin temperatures with strong performance. The optimization involves a thorough consideration of various age-related parameters within both the passive and active systems. This includes factors such as physical parameters, physiological changes, metabolic rates and thermal regulatory mechanisms that are known to differ across different age groups.

The developed model in this study inherits the advantages of the original model with not many input parameters and quick calculation. That is, the model does not need to consider complex local parameters. The user only needs to set the environmental parameters according to the application population and modify the human physical parameters when necessary.

The model innovatively incorporates a holistic optimization of both passive and active parameters, introducing a more interpretable optimization approach for the active parameters by leveraging the TPE algorithm. This algorithm seamlessly combines global search and local fine-tuning characteristics in optimizing the human thermoregulation model. Compared with existing optimization methods, including changing threshold temperature for thermoregulation activities [43,56], optimizing the active system with a genetic algorithm [53] and optimizing only passive parameters but not active parameters [58], the TPE algorithm possesses several advantages: high computational efficiency, the ability to avoid getting stuck in local optima, fine-grained searches once potential optimal regions are found and stronger interpretability by determining the importance of each parameter.

6.2 Limitations and future work

Due to ethical and health considerations, a significant portion of the available data has been collected from older individuals who are in good health. Thus, the model was modified and verified only for healthy elderly people. However, it is important to acknowledge that various health conditions can impact a person's thermoregulatory functions. A database for unhealthy elderly with different levels of frailty requires further consideration.

In this study, the modulation of cardiac and cutaneous blood flow was primarily achieved through the implementation of vasoconstriction and vasodilation mechanisms. However, it is essential to acknowledge the intricate nature of blood circulation within the human body. The regulatory processes extend beyond simple vascular adjustments and encompass various factors, including hormonal influences and individual health conditions. It is imperative to recognize that this research provides a focused perspective on blood flow control, with limitations arising from the limited exploration of detailed mechanisms governing blood circulation.

The validation of the thermoregulation model for the elderly encountered certain limitations that warrant consideration. One notable challenge was the scarcity of comprehensive datasets specifically tailored to the elderly population, which affected the model's ability to generalize across diverse age and BMI groups within this demographic. The reliance on existing literature and limited real-world data for model validation introduced constraints in accurately simulating diverse scenarios. Moving forward, addressing these limitations through the acquisition of more extensive and diverse datasets will be essential for enhancing the overall robustness and applicability of the thermoregulation model for the elderly.

6.3 Application

Human thermophysiological response underpins thermal sensation in transient environments. By comprehensively considering the age-induced thermal response changes within the applicable population, the model is able to provide a more accurate representation of the thermal comfort and energy efficiency requirements for different age groups, particularly the elderly. This information can be invaluable in designing and optimizing various systems, such as building HVAC systems or personal thermal management devices, to ensure optimal comfort and well-being for individuals across the age spectrum. Real-time and long-term monitoring and analysis are efficient methods for securing comfort conditions and may be used in the healthcare sector.

7. Conclusions

With the growing need to improve the quality of life and well-being of the increasing elderly population, this study aimed to develop a thermoregulation model for the Chinese elderly based on an existing one-segment four-node base model for a younger group. By incorporating age-related physical and physiological parameters, the model comprehensively captured and adjusted the model's passive and active parameters. The main findings of the study are shown as follows:

- The demographic representation of the model was verified. A good match between census data and elderly subjects was found, with an average age of 67 and 66 years, respectively. The relative differences between census data and subject data were all lower than 4% in terms of weight, height, BMI and fat percentage. The finding implies the demographic representation of the model to be applied to the Chinese elderly population.

- The influences of passive parameters on mean skin temperature and core temperature were quantified by sensitivity analysis. To take the age-related changes into account, the passive parameters were adjusted to fit the elderly's physiological characteristics. The modified physical parameters include weight, height and fat percentage while the adjusted physiological parameters include BSA, metabolic rate, skin blood flow and cardiac output.
- To optimize the active system, body temperature set points were reset according to thermal responses under neutral thermal environments. The elderly have 0.3˚C lower neutral core temperature. The active parameters were subsequently optimized with the TPE hyperparameter tuning method which is based on Bayesian optimization. The results show lower ARMSE values below 0.4˚C and the optimized active parameters show reduced thermal regulatory responses for the elderly.

The developed model was verified by the published data with temperature ramps. The prediction results show good agreement with the measured data with the RMSE range of 0.10 to 0.35˚C. This research can help to understand the thermal responses of the elderly and can show building managers and operators how to balance thermal comfort and energy efficiency in elderly residences and care homes.

CRediT authorship contribution statement

Shan Zhou: Formal analysis, Investigation, Visualization, Validation, Writing - Original Draft. **Linyuan Ouyang:** Methodology, Software, Data collection, Investigation, Visualization. **Baizhan Li:** Supervision, Conceptualization, Project administration. **Simon Hodder**: Writing

- Review & Editing. **Runming Yao:** Conceptualization, Supervision, Funding acquisition, Writing - Review & Editing.

Declaration of competing interest

The authors declare that they have no known competing financial interests or personal relationships that could have appeared to influence the work reported in this paper.

Data availability

Data will be made available on request.

Acknowledgments

This work was supported by the National Key R&D Program of China [Grant No: 2022YFC3801504] and the Natural Science Foundation of Chongqing, China [Grant No: cstc2021ycjh-bgzxm0156]. The author acknowledges financial support from the Chinese Scholarship Council [No: 202206050102].

References

[1] C. Hughes, S. Natarajan, C. Liu, W.J. Chung, M. Herrera, Winter thermal comfort and health in the elderly, Energy Policy. 134 (2019) 110954. https://doi.org/10.1016/j.enpol.2019.110954.

[2] M.P. Jarzebski, T. Elmqvist, A. Gasparatos, K. Fukushi, S. Eckersten, D. Haase, J. Goodness, S. Khoshkar, O. Saito, K. Takeuchi, T. Theorell, N. Dong, F. Kasuga, R. Watanabe, G.B. Sioen, M. Yokohari, J. Pu, Ageing and population shrinking: implications for sustainability in the urban century, Urban Sustain. 1 (2021) 17. https://doi.org/10.1038/s42949-021-00023-z.

[3] United Nations, World Population Prospects 2022, (2022). https://population.un.org/wpp/Download/Standard/Population/ (accessed December 14, 2022).

[4] J. Chen, Y. Wang, J. Wen, F. Fang, M. Song, The influences of aging population and economic growth on Chinese rural poverty, J. Rural Stud. 47 (2016) 665–676. https://doi.org/10.1016/j.jrurstud.2015.11.002.

[5] R.L. Hwang, C.P. Chen, Field study on behaviors and adaptation of elderly people and their thermal comfort requirements in residential environments, Indoor Air. 20 (2010) 235–245. https://doi.org/10.1111/j.1600-0668.2010.00649.x.

[6] D. Ormandy, V. Ezratty, Thermal discomfort and health: protecting the susceptible from excess cold and excess heat in housing, Adv. Build. Energy Res. 10 (2016) 84–98. https://doi.org/10.1080/17512549.2015.1014845.

[7] Y. Wu, H. Liu, B. Li, R. Kosonen, D. Kong, S. Zhou, R. Yao, Thermal adaptation of the elderly during summer in a hot humid area: Psychological, behavioral, and physiological responses, Energy Build. 203 (2019) 109450. https://doi.org/10.1016/j.enbuild.2019.109450.

[8] J. Yang, I. Nam, J.-R.R. Sohn, The influence of seasonal characteristics in elderly thermal comfort in Korea, Energy Build. 128 (2016) 583–591. https://doi.org/10.1016/j.enbuild.2016.07.037.

[9] C. Hughes, S. Natarajan, Summer thermal comfort and overheating in the elderly, Build. Serv. Eng. Res. Technol. 40 (2019) 426–445. https://doi.org/10.1177/0143624419844518.

[10] A.V. Farahani, J. Jokisalo, N. Korhonen, K. Jylhä, K. Ruosteenoja, R. Kosonen, Overheating risk and energy demand of nordic old and new apartment buildings during average and extreme weather conditions under a changing climate, Appl. Sci. 11 (2021). https://doi.org/10.3390/app11093972.

[11] H.L. Macintyre, C. Heaviside, J. Taylor, R. Picetti, P. Symonds, X.M. Cai, S. Vardoulakis, Assessing urban population vulnerability and environmental risks across an urban area during heatwaves – Implications for health protection, Sci. Total Environ. 610–611 (2018) 678–690. https://doi.org/10.1016/j.scitotenv.2017.08.062.

[12] M.T. Baquero, N. Forcada, Thermal comfort of older people during summer in the continental Mediterranean climate, J. Build. Eng. 54 (2022) 104680. https://doi.org/https://doi.org/10.1016/j.jobe.2022.104680.

[13] N. Forcada, M. Gangolells, M. Casals, B. Tejedor, M. Macarulla, K. Gaspar, Field study on adaptive thermal comfort models for nursing homes in the Mediterranean climate, Energy Build. 252 (2021) 111475. https://doi.org/https://doi.org/10.1016/j.enbuild.2021.111475.

[14] Y. Jiao, H. Yu, Y. Yu, Z. Wang, Q. Wei, Adaptive thermal comfort models for homes for older people in Shanghai, China, Energy Build. 215 (2020) 109918. https://doi.org/10.1016/j.enbuild.2020.109918.

[15] Z. Wang, H. Yu, Y. Jiao, Q. Wei, X. Chu, A field study of thermal sensation and neutrality in free-running aged-care homes in Shanghai, Energy Build. 158 (2018) 1523–1532. https://doi.org/10.1016/j.enbuild.2017.11.050.

[16] W. Zheng, T. Shao, Y. Lin, Y. Wang, C. Dong, J. Liu, A field study on seasonal adaptive thermal comfort of the elderly in nursing homes in Xi'an, China, Build. Environ. 208 (2022) 108623. https://doi.org/https://doi.org/10.1016/j.buildenv.2021.108623.

[17] M.T. Baquero Larriva, A.S. Mendes, N. Forcada, The effect of climatic conditions on occupants' thermal comfort in naturally ventilated nursing homes, Build. Environ. 214 (2022) 108930. https://doi.org/https://doi.org/10.1016/j.buildenv.2022.108930.

[18] A. Gasparrini, Y. Guo, M. Hashizume, E. Lavigne, A. Zanobetti, J. Schwartz, A. Tobias, S. Tong, J. Rocklöv, B. Forsberg, M. Leone, M. De Sario, M.L. Bell, Y.-L.L.Y.Y.-L.L. Guo, C.-F. Wu, H. Kan, S.-M. Yi, M. De Sousa Zanotti Stagliorio Coelho, P.H.N. Saldiva, Y. Honda, H. Kim, B. Armstrong, M. De Sario, M.L. Bell, Y.-L.L.Y.Y.-L.L. Guo, C.-F. Wu, H. Kan, S.-M. Yi, M. de S.Z.S. Coelho, P.H.N. Saldiva, Y. Honda, H. Kim, B. Armstrong, Mortality risk attributable to high and low ambient temperature: a multicountry observational study, Lancet. 386 (2015) 369–375. https://doi.org/10.1016/s0140-6736(14)62114-0.

[19] Y. Jiang, Z. Wang, B. Lin, D. Mumovic, Development of a health data-driven model for a thermal comfort study, Build. Environ. 177 (2020) 106874. https://doi.org/10.1016/j.buildenv.2020.106874.

[20] K. Tsuzuki, T. Ohfuku, Thermal sensation and thermoregulation in elderly compared to young people in Japanese winter season, Proc. Indoor Air. (2002) 659–664.

[21] C. Bae, H. Lee, C. Chun, Predicting indoor thermal sensation for the elderly in welfare centres in Korea using local skin temperatures, Indoor Built Environ. 26 (2017) 1155–1167. https://doi.org/10.1177/1420326x16664563.

[22] C. Yu, B. Li, Y. Wu, B. Chen, R. Kosonen, S. Kilpelainen, H. Liu, Performances of machine learning algorithms for individual thermal comfort prediction based on data from professional and practical settings, J. Build. Eng. 61 (2022) 105278. https://doi.org/https://doi.org/10.1016/j.jobe.2022.105278.

[23] B. Tejedor, M. Casals, M. Gangolells, M. Macarulla, N.N. Forcada, Human comfort modelling for elderly people by infrared thermography: Evaluating the thermoregulation system responses in an indoor environment during winter, Build. Environ. 186 (2020) 107354. https://doi.org/10.1016/j.buildenv.2020.107354.

[24] S. Konz, C. Hwang, B. Dhiman, J. Duncan, A. Masud, An experimental validation of mathematical simulation of human thermoregulation, Comput. Biol. Med. 7 (1977) 71–82. https://doi.org/https://doi.org/10.1016/0010-4825(77)90007-5.

[25] M.P. Castellani, T.P. Rioux, J.W. Castellani, A.W. Potter, X. Xu, A geometrically accurate 3 dimensional model of human thermoregulation for transient cold and hot environments, Comput. Biol. Med. 138 (2021) 104892. https://doi.org/https://doi.org/10.1016/j.compbiomed.2021.104892.

[26] J. Yang, F. Wang, M.D. White, R. Li, G. Song, C. V Etter, E.A. Gnatiuk, A.S. Perrotta, A 7-segment numerical hand-glove/mitten model for predicting thermophysiological responses of the human hand in extremely cold conditions, Comput. Biol. Med. 151 (2022) 106351. https://doi.org/https://doi.org/10.1016/j.compbiomed.2022.106351.

[27] Q. Deng, J. Zhao, W. Liu, Y. Li, Heatstroke at home: Prediction by thermoregulation modeling, Build. Environ. 137 (2018) 147–156. https://doi.org/https://doi.org/10.1016/j.buildenv.2018.04.017.

[28] M. Yokota, L. Berglund, S. Cheuvront, W. Santee, W. Latzka, S. Montain, M. Kolka, D. Moran, Thermoregulatory model to predict physiological status from ambient environment and heart rate, Comput. Biol. Med. 38 (2008) 1187–1193. https://doi.org/https://doi.org/10.1016/j.compbiomed.2008.09.003.

[29] A.P. Welles, X. Xu, W.R. Santee, D.P. Looney, M.J. Buller, A.W. Potter, R.W. Hoyt, Estimation of core body temperature from skin temperature, heat flux, and heart rate using a Kalman filter, Comput. Biol. Med. 99 (2018) 1–6. https://doi.org/https://doi.org/10.1016/j.compbiomed.2018.05.021.

[30] S. Zhou, B. Li, C. Du, H. Liu, Y. Wu, S. Hodder, M. Chen, R. Kosonen, R. Ming, L. Ouyang, R. Yao, Opportunities and challenges of using thermal comfort models for building design and operation for the elderly: A literature review, Renew. Sustain. Energy Rev. 183 (2023) 113504. https://doi.org/https://doi.org/10.1016/j.rser.2023.113504.

[31] M. Fu, W. Weng, W. Chen, N. Luo, Review on modeling heat transfer and thermoregulatory responses in human body, J. Therm. Biol. 62 (2016) 189–200. https://doi.org/https://doi.org/10.1016/j.jtherbio.2016.06.018.

[32] K. Katić, R. Li, W. Zeiler, Thermophysiological models and their applications: A review, Build. Environ. 106 (2016) 286–300. https://doi.org/https://doi.org/10.1016/j.buildenv.2016.06.031.

[33] L. Ji, A. Laouadi, C. Shu, L. Wang, M.A. Lacasse, Evaluation and improvement of the thermoregulatory system for the two-node bioheat model, Energy Build. 249 (2021) 111235. https://doi.org/10.1016/j.enbuild.2021.111235.

[34] P.O. Fanger, Thermal comfort: Analysis and Applications in Environmental Engineering, Danish Technical Press, Copenhagen, 1970.

[35] ASHARE, ANSI/ASHRAE Standard 55-2020 Thermal Environmental Conditions for Human Occupancy, (2020).

[36] S. Zhang, Z. Lin, Predicted Mean Vote with skin temperature from standard effective temperature model, Build. Environ. 183 (2020) 107133. https://doi.org/10.1016/j.buildenv.2020.107133.

[37] R. Ming, B. Li, C. Du, W. Yu, H. Liu, R. Kosonen, R. Yao, A comprehensive understanding of adaptive thermal comfort in dynamic environments – An interaction matrix-based path analysis modeling framework, Energy Build. 284 (2023) 112834. https://doi.org/10.1016/j.enbuild.2023.112834.

[38] C. Du, B. Li, H. Liu, Y. Wei, M. Tan, Quantifying the cooling efficiency of air velocity by heat loss from skin surface in warm and hot environments, Build. Environ. 136 (2018) 146–155. https://doi.org/10.1016/j.buildenv.2018.03.023.

[39] Q. Wu, J. Liu, L. Zhang, J. Zhang, L. Jiang, Study on thermal sensation and thermal comfort in environment with moderate temperature ramps, Build. Environ. 171 (2020) 106640. https://doi.org/10.1016/j.buildenv.2019.106640.

[40] A.P. Gagge, J.A.J. Stolwijk, Y. Nishi, An Effective Temperature Scale Based on a Simple Model of Human Physiological Regulatiry Response, ASHRAE Trans. 13 (1971) 21–36.

[41] A.P. Gagge, A.P. Fobelets, L.G. Berglund, A standard predictive index of human response to the thermal environment, ASHRAE Trans. 92 (1986).

[42] A.P. Gagge, J.A.J. Stolwijk, J.D. Hardy, Comfort and thermal sensations and associated physiological responses at various ambient temperatures, Environ. Res. 1 (1967) 1–20.

[43] L. Ji, A. Laouadi, L. Wang, M.A. Lacasse, Development of a bioheat model for older people under hot and cold exposures, Build. Simul. 15 (2022) 1815–1829. https://doi.org/10.1007/s12273-022-0890-3.

[44] F. Davoodi, H. Hasanzadeh, S. Alireza Zolfaghari, M. Maerefat, Developing a new individualized 3-node model for evaluating the effects of personal factors on thermal sensation, J. Therm. Biol. 69 (2017) 1–12. https://doi.org/10.1016/j.jtherbio.2017.05.004.

[45] A. Zolfaghari, M. Maerefat, A new simplified thermoregulatory bioheat model for evaluating thermal response of the human body to transient environments, Build. Environ. 45 (2010) 2068–2076. https://doi.org/10.1016/j.buildenv.2010.03.002.

[46] F. Davoodi, H. Hassanzadeh, S.A. Zolfaghari, G. Havenith, M. Maerefat, A new individualized thermoregulatory bio-heat model for evaluating the effects of personal characteristics on human body thermal response, Build. Environ. 136 (2018) 62–76. https://doi.org/10.1016/j.buildenv.2018.03.026.

[47] J.A.J. Stolwijk, A mathematical model of physiological temperature regulation in man, Washington, D.C., 1971.

[48] D. Fiala, Dynamic simulation of human heat transfer and thermal comfort, De Montfort University, 1998.

[49] D. Fiala, K.J. Lomas, M. Stohrer, A computer model of human thermoregulation for a wide range of environmental conditions: the passive system., J. Appl. Physiol. 87 (1999) 1957–1972. https://doi.org/10.1152/jappl.1999.87.5.1957.

[50] D. Fiala, G. Havenith, P. Bröde, B. Kampmann, G. Jendritzky, UTCI-Fiala multi-node model of human heat transfer and temperature regulation, Int. J. Biometeorol. 56 (2012) 429–441. https://doi.org/10.1007/s00484-011-0424-7.

[51] S.I. Tanabe, K. Kobayashi, J. Nakano, Y. Ozeki, M. Konishi, Evaluation of thermal comfort using combined multi-node thermoregulation (65MN) and radiation models and computational fluid dynamics (CFD), Energy Build. 34 (2002) 637–646. https://doi.org/https://doi.org/10.1016/S0378-7788(02)00014-2.

[52] C. Huizenga, Z. Hui, E. Arens, A model of human physiology and comfort for assessing complex thermal environments, Build. Environ. 36 (2001) 691–699. https://doi.org/https://doi.org/10.1016/S0360-1323(00)00061-5.

[53] D.T. Novieto, Adapting a human thermoregulation model for predicting the thermal response of older persons, De Montfort University, 2013.

[54] Y. Takahashi, A. Nomoto, S. Yoda, R. Hisayama, M. Ogata, Y. Ozeki, S. Tanabe, Thermoregulation model JOS-3 with new open source code, Energy Build. 231 (2021) 110575. https://doi.org/https://doi.org/10.1016/j.enbuild.2020.110575.

[55] M. Rida, N. Ghaddar, K. Ghali, J. Hoballah, Elderly bioheat modeling: changes in physiology, thermoregulation, and blood flow circulation, Int. J. Biometeorol. 58 (2014) 1825–1843. https://doi.org/10.1007/s00484-013-0785-1.

[56] M. Itani, N. Ghaddar, K. Ghali, A. Laouadi, Bioheat modeling of elderly and young for prediction of physiological and thermal responses in heat-stressful conditions, J. Therm. Biol. 88 (2020) 102533. https://doi.org/10.1016/j.jtherbio.2020.102533.

[57] A. Hirata, T. Nomura, I. Laakso, Computational estimation of body temperature and sweating in the aged during passive heat exposure, Int. J. Therm. Sci. 89 (2015) 154–163. https://doi.org/https://doi.org/10.1016/j.ijthermalsci.2014.11.001.

[58] T. Ma, J. Xiong, Z. Lian, A human thermoregulation model for the Chinese elderly, J. Therm. Biol. 70 (2017) 2–14. https://doi.org/10.1016/j.jtherbio.2017.08.002.

[59] A. Coccarelli, H.M. Hasan, J. Carson, D. Parthimos, P. Nithiarasu, Influence of ageing on human body blood flow and heat transfer: A detailed computational modelling study, Int. j. Numer. Method. Biomed. Eng. 34 (2018) 1–21. https://doi.org/10.1002/cnm.3120.

[60] B. Li, Y. Yang, R. Yao, H. Liu, Y. Li, A simplified thermoregulation model of the human body in warm conditions, Appl. Ergon. 59 (2017) 387–400. https://doi.org/10.1016/j.apergo.2016.09.010.

[61] H.H. Pennes, Analysis of Tissue and Arterial Blood Temperatures in the Resting Human Forearm, J. Appl. Physiol. 1 (1948) 93–122. https://doi.org/10.1152/jappl.1948.1.2.93.

[62] Y. Yang, B. Li, H. Liu, M. Tan, R. Yao, A study of adaptive thermal comfort in a well-controlled climate chamber, Appl. Therm. Eng. 76 (2015) 283–291. https://doi.org/10.1016/j.applthermaleng.2014.11.004.

[63] Y. Wu, Z. Zhang, H. Liu, B. Li, B. Chen, R. Kosonen, J. Jokisalo, Age differences in thermal comfort and physiological responses in thermal environments with temperature ramp, Build. Environ. 228 (2023) 109887. https://doi.org/10.1016/j.buildenv.2022.109887.

[64] S. Zhou, B. Li, C. Du, R. Yao, L. Ouyang, H. Zhou, R. Kosonen, A.K. Melikov, L. Shang, H. Liu, Developing thermal prediction models for the elderly under temperature step changes, Build. Environ. 245 (2023) 110902. https://doi.org/https://doi.org/10.1016/j.buildenv.2023.110902.

[65] H. Liu, Y. Wu, B. Li, Y. Cheng, R. Yao, Seasonal variation of thermal sensations in residential buildings in the Hot Summer and Cold Winter zone of China, Energy Build. 140 (2017) 9–18. https://doi.org/10.1016/j.enbuild.2017.01.066.

[66] W. Liu, Z. Lian, Q. Deng, Y. Liu, Evaluation of calculation methods of mean skin temperature for use in thermal comfort study, Build. Environ. 46 (2011) 478–488. https://doi.org/10.1016/j.buildenv.2010.08.011.

[67] R.E. Patterson, L.L. Frank, A.R. Kristal, E. White, A comprehensive examination of health conditions associated with obesity in older adults, Am. J. Prev. Med. 27 (2004) 385–390. https://doi.org/10.1016/j.amepre.2004.08.001.

[68] National Bureau of Statistics of China, National data, (2022). https://data.stats.gov.cn/easyquery.htm?cn=C01 (accessed April 4, 2023).

[69] General Administration of Sport of China, The fifth national physical fitness monitoring bulletin, (2022). https://www.sport.gov.cn/n315/n329/c24335066/content.html (accessed April 4, 2023).

[70] T. Wei, A review of sensitivity analysis methods in building energy analysis, Renew. Sustain. Energy Rev. 20 (2013) 411–419. https://doi.org/10.1016/j.rser.2012.12.014.

[71] L.A. Holowatz, W.L. Kenney, Peripheral mechanisms of thermoregulatory control of skin blood flow in aged humans., J. Appl. Physiol. 109 (2010) 1538–1544. https://doi.org/10.1152/japplphysiol.00338.2010.

[72] M. Itani, N. Ghaddar, K. Ghali, A. Laouadi, Development of heat stress charts for older people under indoor environmental conditions, Energy Build. 224 (2020) 110274. https://doi.org/https://doi.org/10.1016/j.enbuild.2020.110274.

[73] Y. Tochihara, K. Yamashita, K. Fujii, Y. Kaji, H. Wakabayashi, H. Kitahara, Thermoregulatory and cardiovascular responses in the elderly towards a broad range of gradual air temperature changes, J. Therm. Biol. 99 (2021). https://doi.org/10.1016/j.jtherbio.2021.103007.

[74] C.M. Blatteis, Age-Dependent Changes in Temperature Regulation - A Mini Review, Gerodontology. 58 (2012) 289–295. https://doi.org/10.1159/000333148.

[75] J.K. Vanos, J.S. Warland, T.J. Gillespie, N.A. Kenny, Thermal comfort modelling of body temperature and psychological variations of a human exercising in an outdoor environment, Int J Biometeorol. 56 (2012) 21–32. https://doi.org/10.1007/s00484-010-0393-2.

[76] Y. Tang, H. Yu, Z. Wang, M. Luo, C. Li, Validation of the Stolwijk and Tanabe human thermoregulation models for predicting local skin temperatures of older people under thermal transient conditions, Energies. 13 (2020) 6524. https://doi.org/10.3390/en13246524.

[77] J. Bergstra, R. Bardenet, Y. Bengio, B. Kégl, Algorithms for Hyper-Parameter Optimization, in: Proc. 24th Int. Conf. Neural Inf. Process. Syst., Curran Associates Inc., Red Hook, NY, USA, 2011: pp. 2546–2554.